§7. Particle Transport Characterization by Line-integrated Phase Contrast Measurements on LHD

Vyacheslavov, L.N. (Budker Institute of Nuclear Physics), Tanaka, K., Michael, C.A. (JSPS Fellow)

Anomalous transport governs particle and energy loses in most magnetic fusion devices including LHD [1]. Fluctuation induced particle and energy anomalous transports are determined by temporally averaged products of local radial fluctuations of plasma density $\tilde{n}_r$, velocity $\tilde{v}_r$, and temperature fluctuations $\tilde{T}$: $\Gamma = \langle \tilde{n}_r \tilde{v}_r \rangle$, $Q = n\langle \tilde{v}_r \tilde{T} \rangle + T\langle \tilde{n}_r \tilde{v}_r \rangle$. For evaluation of balance of particles and energy, values of Γ and Q integrated over entire flux surfaces are required. Up to now there are no diagnostics capable to cover with local measurements of $\tilde{n}_r, \tilde{v}_r$ the whole cross-section of hot dense plasma. Yet, techniques using active electromagnetic probe beams like phase contrast or interferometry can extend the observation region to considerable fraction of the plasma cross-section. These techniques have fine spatial resolution in the direction normal to probe beam but data are line-integrated $\tilde{N} = \int \tilde{n} dz$ (see figure 1). Figure 1 shows geometry where probe beam passes though the plasma edge. In this case, the major contribution to signal is produced by radial component of fluctuations $\tilde{N} \approx \tilde{N}_r = \int \tilde{n}_r dz$. The phase contrast imaging [2] with 32ch linear detector array is employed in our experiment. Making use of fines both temporal and spatial resolutions it is possible to calculate the instant velocity $\tilde{V}_R$ of characteristic structures in line integrated density fluctuations $\tilde{N}$. For determination of $\tilde{V}$ we utilize the spatial shift technique, which is similar to time delay method used previously (for example in [3]) but it is applied in spatial domain rather than in time domain. This results in better temporal resolution relative to the time delay technique. The question arises how the averaged transport $\overline{\Gamma a} = \langle \tilde{N} \tilde{V}_R \rangle$ determined from the line integrated data relates to true transport $\overline{\Gamma} = \langle \int \tilde{n}_r \tilde{v}_r \rangle$. For simple test of the method we simulate plasma as a stack of 10 independent flat layers of wave-like density fluctuations with random $\tilde{n}_r$ and $\tilde{v}_r$, directed along the layers. Correlation between $\tilde{n}_r$ and $\tilde{v}_r$ in each layer is simultaneously modulated and varies from 0.5 to 0. For this model function both $\overline{\Gamma}$ and $\overline{\Gamma a}$ are calculated and shown in figure 2. Flux $\overline{\Gamma a}$ obtained from line-integrated data is more noisy and has lower amplitude than the true flux $\overline{\Gamma}$ due to the loss of correlation between density and velocity of fluctuation still it keeps the same time behavior as true flux. Application of this technique to high β plasma discharge is shown in figure 3. Here $\overline{\Gamma a}$ is plotted for discharges #74926 (upper trace) and #74937 (lower trace) and for plasma region outside LCFS (left fraction of the probe beam in figure 1), where still exists large n_e~30%$n_e$max. The positive (directed outside) particle flux decreases temporally after TESPEL (tracer encapsulated solid pellet) injection and later again after two of four NBIs are stopped. Then turbulent flux starts to rise after third NBI stops. These first results show a new possibility to get information on turbulent particle flux integrated over large plasma surface.

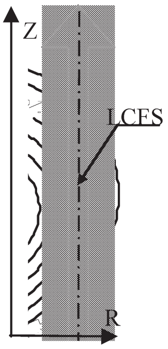

Fig.1. Geometry of phase contrast measurements with the probe beam (grey arrow) center localized at the last close flux surface.

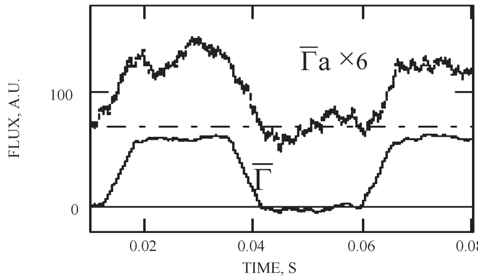

Fig.2 Fluxes $\overline{\Gamma}$ and $\overline{\Gamma a}$ calculated for model structure of 10 independent flat turbulent layers

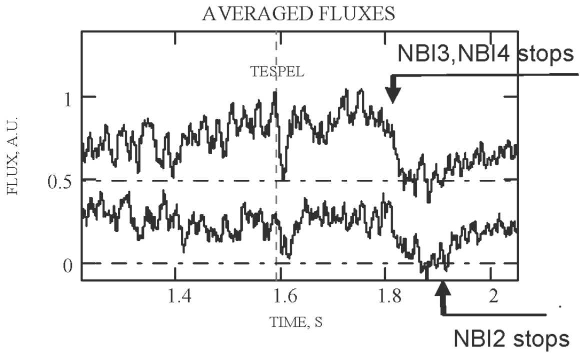

Fig 3. Particle flux $\overline{\Gamma a}$ calculated from measurements on high β discharges #74926 (upper trace) and #74937 (lower trace)

References

1) Tanaka, K. et al., Nucl. Fus. **46**, 110 (2006)
2) Tanaka, K. et al., Rev. Sci. Instrum. **74**, 1633 (2003)
3) M. Jakubowski et al., Rev. Sci. Instrum. **70**, 874 (1999)